# Degree of bending in steel tubular T-joints with concrete-filled chords subjected to axial loadings

Hamid Ahmadi<sup>\*1</sup> and Mahdi Ghorbani<sup>2</sup>

<sup>1</sup>National Centre for Maritime Engineering and Hydrodynamics, Australian Maritime College (AMC), University of Tasmania, Launceston, TAS 7248, Australia <sup>2</sup>Faculty of Civil Engineering, University of Tabriz, Tabriz 5166616471, Iran

(Received April 21, 2025, Revised June 30, 2025, Accepted July 2, 2025)

**Abstract.** Through-the-thickness stress distribution in a tubular member has a profound effect on the fatigue behavior of tubular joints commonly found in steel offshore structures. Such stress distribution can be characterized by the degree of bending (DoB). Although tubular T-joints with concrete-filled chords are commonly used in offshore tubular structures and the concrete fill can have a significant effect on the DoB values at the brace-to-chord intersection, no investigation has been reported on the DoB in tubular T-joints with concrete-filled chords due to the complexity of the problem and high cost involved. In the present research, data extracted from 162 stress analyses conducted on 81 finite element (FE) models subjected to brace tension and compression, verified based on available experimental data and parametric equations, was used to study the effects of geometrical parameters on the DoB values in tubular T-joints with concrete-filled chords. Parametric FE study was followed by a set of nonlinear regression analyses to develop four new DoB parametric equations for the fatigue analysis and design of axially loaded tubular T-joints with concrete-filled chords.

**Keywords:** degree of bending (DoB); fatigue; offshore jacket structure; tubular T-joint with concrete-filled chord

#### 1. Introduction

The jacket-type platform stands as the most prevalent fixed offshore structure chosen for the extraction of oil and gas from beneath the seabed's hydrocarbon reservoirs. The central structural system of such an offshore platform, namely the jacket substructure (Fig. 1(a)), is assembled from tubular components, where one end of the branch members, referred to as braces, are welded to the primary member, known as the chord. This welding process produces what is commonly called a tubular joint (Fig. 1(b)). If the load-bearing capacity of a tubular joint is found to be inadequate during the design stage, e.g., the chord thickness requirement is beyond the forming limits of fabricators, it can be enhanced by introducing concrete to the inside of the chord (Musa *et al.* 2018) or other stiffening methods such as implementing collar plates (Nassiraei *et al.* 2019, 2025b), doubler plates (Nassiraei and Arab 2024), and outer plates (Nassiraei and Yara 2022, 2023). Tubular joints are also prone to fatigue-related damage throughout their operational lifespan due to

ISSN: 2093-6702 (Print), 2093-677X (Online)

<sup>\*</sup>Corresponding author, Ph.D., E-mail: hamid.ahmadi@utas.edu.au

the creation and propagation of cracks induced by cyclic loads stemming from wave action.

The stress-life (S-N) methodology, embraced by prominent offshore design codes and standards like API RP 2A (2007), DNV OS C201 (2008), and DNV RP C203 (2005), is widely utilized for predicting the fatigue life of tubular joints, primarily relying on hot-spot stress (HSS) calculations. Neveraluess, extensive analysis of fatigue test data has revealed that tubular joints, even with similar HSS values, can exhibit significantly varying cycles to failure when they differ in geometry or loading conditions (Connolly 1986). These differences are believed to stem from alterations in crack propagation rates, influenced by the through-the-thickness stress distribution, which can be quantified using the degree of bending (DoB). DoB is defined as the ratio of bending stress to the total stress.

Fig. 2 depicts the typical stress distribution through the chord wall of a tubular joint. Through-the-thickness stress field is a combination of the linear stress due to the chord wall bending and the nonlinear stress concentration at the weld toe due to the section change at the intersection. The nonlinear stress distribution around the weld toe is dependent on the weld geometry and is difficult to predict during the design stage. Since for a deep crack, the weld-toe stress concentration has a relatively little effect on the through-the-thickness stress field (Chang and Dover 1999), the stress distribution across the wall thickness is usually assumed to be a linear combination of membrane and bending stresses. Hence, the DoB can be expressed as follows

$$DoB = \frac{\sigma_B}{\sigma_T} = \frac{\sigma_B}{\sigma_B + \sigma_M} \tag{1}$$

where  $\sigma_T$  is total stress; and  $\sigma_B$  and  $\sigma_M$  are the bending and membrane stresses, respectively.

Under any specific loading condition, the DoB value along the weld toe of a tubular joint is mainly determined by the joint geometry. To study the behavior of a tubular joint and to easily relate this behavior to the geometrical characteristics of the joint, a set of dimensionless geometrical parameters has been defined. Fig. 1(b) depicts a tubular T-joint with concrete-filled chord and the geometrical parameters  $\tau$ ,  $\gamma$ ,  $\beta$ ,  $\alpha$ , and  $\alpha$ <sub>B</sub> for chord and brace diameters D and D, their corresponding wall thicknesses D and D, and respective lengths D and D. Critical positions along the weld toe of the brace-to-chord intersection for the calculation of the DoB values in a tubular T-joint, i.e., saddle and crown, are shown in Fig. 1(b).

Previous studies have shown that the standard stress-life approach may be unconservative for the joints with low DoB. For example, the results of the tubular joint fatigue tests conducted by Eide *et al.* (1993) confirmed the detrimental effect of low DoB on fatigue life. It was found that the experimentally measured fatigue life is significantly shorter compared to the prediction using the S-N curve method. According to Chang and Dover (1999), finite element analyses of tubular joints have shown that typical DoB values are in the range of 0.8–0.9 for the joints used to derive the S-N curves. Smaller values can be considered as low DoB. For the double T specimens studied by Eide *et al.* (1993), a DoB of 0.69 was measured. Hence, to obtain a more accurate fatigue life prediction, the current standard HSS-based S-N approach should be modified to include the effect of DoB.

The other shortcoming of the S-N approach is that this method gives only the total life and cannot be used to predict fatigue crack growth and the remaining life of cracked joints. For the fatigue analysis of cracked joints, fracture mechanics (FM) should be used. The accurate determination of the stress intensity factor (SIF) is the key for FM calculations. Owing to the complexities introduced by the structural geometry and the nature of the local stress fields, it is impossible to calculate the SIFs analytically. This problem is often tackled by using simplified

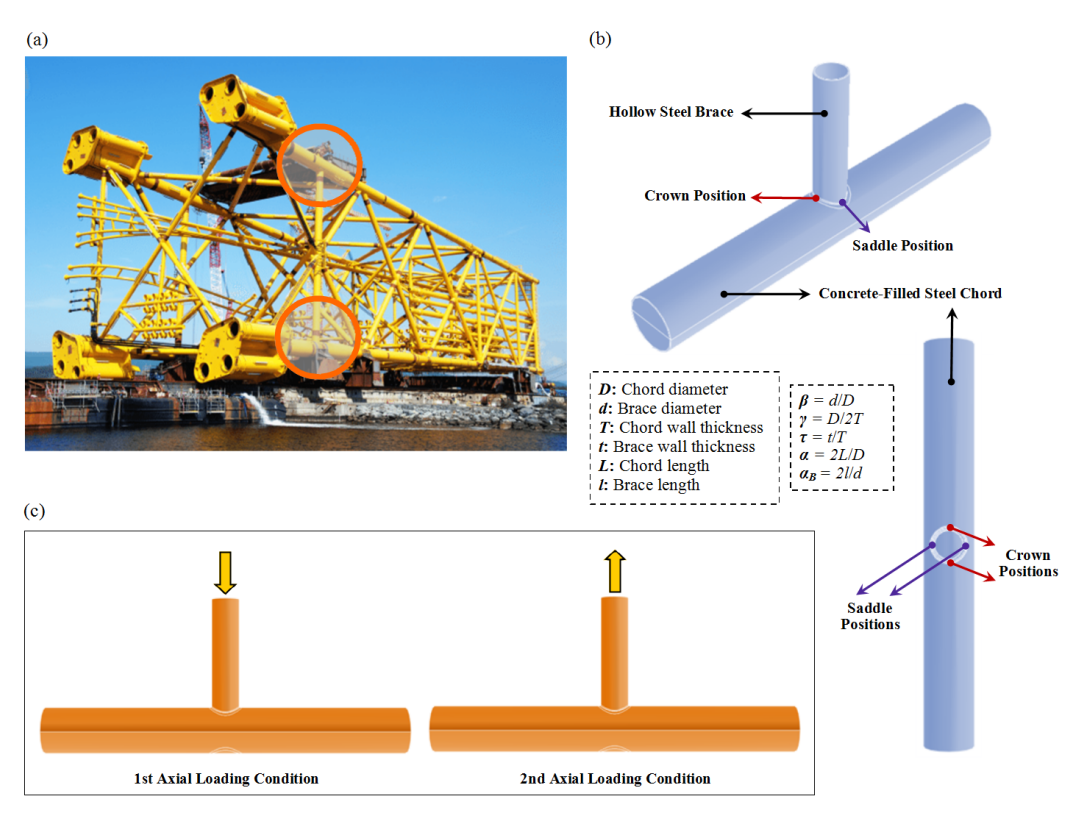


Fig. 1 (a) Tubular T-joints in an offshore jacket structure, (b) Geometrical notation for a tubular T-joint with concrete-filled chord and (c) Studied axial loading conditions

models, such as the flat plate solution (Newman and Raju 1986) or methods based on the T-Butt weight function (Chang 1997), with an appropriate load shedding model. For example, to approximate the SIF value for a tubular joint using T-butt solutions, Eq. (2) can be used (Lee and Bowness 2002).

$$SIF = [Mk_m M_m SCF(1 - DoB) + Mk_b M_b SCF.(DoB)] \sigma_n \sqrt{\pi a}$$
(2)

where a denotes the crack depth,  $\sigma_n$  is the nominal stress, Mk is the weld-toe magnification factor, M is the plain plate shape factor, SCF is the stress concentration factor, and subscripts m and b denote membrane and bending loadings, respectively.

Eq. (2) indicates that to use simplified SIF models for the calculation of remaining fatigue life of tubular joints, the information is required again on the distribution of through-the-thickness stress acting on the anticipated crack path, which can be characterized by the DoB.

The above discussion clearly demonstrates that DoB is an important input parameter for the calculation of fatigue crack growth and estimation of fatigue life in tubular welded joints. Since early 1990s, several research works have been devoted to the study of the DoB in simple tubular connections such as unstiffened T-, K-, and X-joints. As a result, a set of parametric design formulas in terms of the joint's geometrical parameters have been proposed providing the DoB values at certain positions adjacent to the weld for several loading conditions. However, for

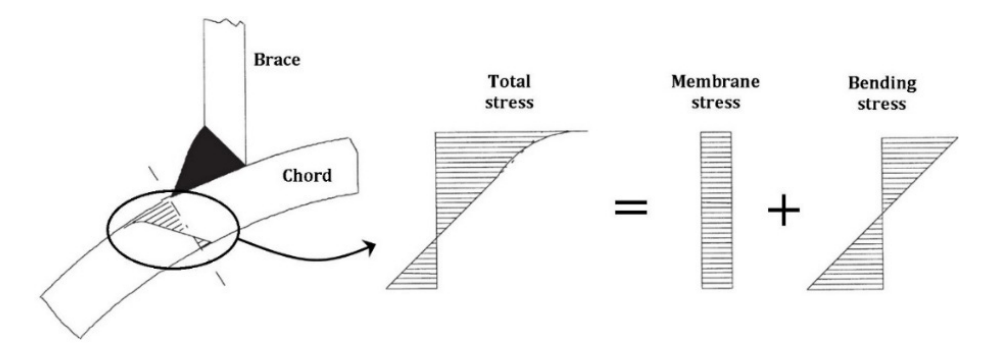


Fig. 2 Through-the-thickness stress distribution in the chord member of a tubular joint

stiffened tubular joints, much fewer investigations have been reported, and no research work is currently available in the literature on the DoB of tubular joints with concrete-filled chords.

In the present paper, results of a numerical investigation on DoB values in tubular T-joints with concrete-filled chords are presented and discussed. In this research program, a set of parametric finite element (FE) stress analyses was carried out on 81 reinforced tubular T-joint models subjected to two types of axial loading (Fig. 1(c)). In-plane bending (IPB) and out-of-plane bending (OPB) moment loadings are not covered in the present research. Analysis results were used to present general remarks on the effects of geometrical parameters including  $\tau$  (brace-to-chord thickness ratio),  $\gamma$  (chord wall slenderness ratio),  $\beta$  (brace-to-chord diameter ratio), and  $\alpha$  (chord length-to-radius ratio) on DoB values at the saddle and crown positions. Based on the results of reinforced T-joint FE models, verified using available experimental data and parametric equations, a DoB database was prepared. Afterwards, a new set of DoB parametric equations was established, based on nonlinear regression analyses, for the fatigue analysis and design of tubular T-joints with concrete-filled chords subjected to brace tension and compression. The reliability of proposed equations was evaluated according to the acceptance criteria recommended by the UK Department of Energy (1983).

#### 2. Literature review

Morgan and Lee (1998) derived mean and design equations for DoB values at critical positions in axially loaded tubular K-joints from a previously established FE database of 254 joints. Design equations met all the acceptance criteria recommended by the UK Department of Energy (1983). Chang and Dover (1999) carried out a series of systematic thin-shell FE analyses for 330 tubular X- and DT-joints typically found in offshore structures under six different types of loading. Based on the results of nearly 2000 FE analyses, a set of parametric equations was developed to calculate the DoB at critical positions.

Lee and Bowness (2002) proposed an engineering methodology for estimating SIF solutions for semi-elliptical weld-toe cracks in tubular joints. The methodology uses the T-butt solutions proposed previously by the authors in conjunction with the SCFs and the DoB values in uncracked tubular joints. Shen and Choo (2012) determined the SIFs for a grouted tubular joint. They found that the fatigue strength of a grouted joint may be lower than that of as-welded joint, because when

normalized with the HSS, the shape factor of grouted joint is higher than that of original as-welded joint due to the reduction in the DoB caused by the presence of in-filled grout in the chord. For grouted tubular joints, it is essential to consider the effect of DoB in practical fatigue assessment using HSS approach.

Ahmadi et al. (2015) performed a set of parametric stress analyses on 81 K-joint FE models subjected to two different types of IPB moment loading. Analysis results were used to present general remarks on the effect of geometrical parameters on the DoB values at the toe and heel positions; and a new set of DoB parametric equations was developed. Ahmadi and Asoodeh (2016) analyzed 81 K-joint FE models subjected to two types of OPB moment loading. Results were used to study the geometrical effects on the DoB at the saddle position; and two new DoB design formulas were proposed. Ahmadi and Asoodeh (2015) studied the DoB in uniplanar tubular KT-joints of jacket structures subjected to axial loads. Their study was limited to the central brace DoB values and no design equation was proposed for the DoB along the weld toe of the outer braces. Also, IPB and OPB loadings were not included.

Ahmadi and Ghaffari (2015b) proposed a set of probability density functions for the DoB in tubular X-joints subjected to four types of bending loads including two types of IPB and two types of OPB moment loading. Ahmadi and Ghaffari (2015a) developed probability distribution models for the DoB and SIF values in axially loaded tubular K-joints. Ahmadi and Amini Niaki (2019) studied the degree of bending in two-planar tubular DT-joints under axial and bending loads. They developed a set of parametric equations to predict the DoB values at the saddle and crown positions. Ahmadi (2019) established a probability distribution model for the degree of bending in axially loaded tubular KT-joints.

Data extracted from 648 FE analyses carried out on 81 tubular KT-joint models was used by Ahmadi and Zavvar (2020) to study the effects of geometrical parameters on the DoB values in KT-joints subjected to eight different types of axial, IPB, and OPB loadings. Generated FE models were validated using experimental data, previous FE results, and available parametric equations. Geometrically parametric investigation was followed by a set of nonlinear regression analyses to develop 21 parametric design formulas for the calculation of the DoB in tubular KT-joints under the axial, IPB, and OPB loadings.

Ahmadi et al. (2020) developed a set of fatigue design equations for the calculation of DoB values in multi-planar tubular XT-joints of offshore jacket-type platforms subjected to axial loading. Ahmadi and Alizadeh Atalo (2021) investigated the effect of geometrical parameters on the degree of bending in multi-planar tubular KK-joints of the jacket substructure in an offshore wind turbine. Ahmadi and Ghorbani (2023) proposed six DoB parametric equations for the fatigue analysis and design of axially loaded two-planar DYT-joints. Nassiraei et al. (2025a) studied the DoB in tubular X-joints retrofitted with various types of fiber-reinforced polymers subjected to axial loading.

Based on the above discussion, it can be concluded that despite the comprehensive research carried out on the study of SCFs Efthymiou (1988), Ahmadi et al. (2012), Ahmadi and Zavvar (2016), Sadat Hosseini et al. (2021), and Ahmadi and Imani (2022) among others], SIFs (Shao 2006) among others], local joint flexibility (LJF) Ahmadi and Ziaei Nejad (2017a, b), Nassiraei (2020a, b), Ahmadi and Mohammadpourian Janfeshan (2021), and Nassiraei (2025) among others], and ultimate strength Azari-Dodaran et al. (2018), Azari-Dodaran and Ahmadi (2019), and Nassiraei (2023) among others], the research works on the DoB in tubular joints are scarce and the studied joint types are limited to simple connections. Moreover, it is evident that despite frequent application of T-joints with concrete-filled chords in the design of offshore jacket structures, the

DoB in such joints has not been studied so far and no parametric equation is currently available for the DoB calculation in concrete-filled tubular T-joints.

## FE modeling and analysis of tubular T-joints with concrete-filled chords for the DoB calculation

FE-based software package ABAQUS Ver. 2021 was used in present research for the modeling and analysis of tubular T-joints with concrete-filled chords, subjected to two types of axial loading depicted in Fig. 1(c), to extract the DoB values for parametric study and formulation. This section presents the details of FE modeling and analysis.

## 3.1 Simulation of the weld profile

Accurate modeling of the weld profile is one of the important factors affecting the accuracy of the DoB results. In the present research, the welding size along the brace-to-chord intersection satisfies the AWS D 1.1 (2002) specifications. The weld sizes at the crown and saddle positions can be determined as follows

$$H_{w}(\text{mm}) = 0.85t(\text{mm}) + 4.24$$

$$L_{w} = \frac{t}{2} \left[ \frac{135^{\circ} - \psi \text{ (deg.)}}{45^{\circ}} \right]$$

$$\psi = \begin{cases} 90^{\circ} & \text{Crown} \\ 180^{\circ} - \cos^{-1}\beta \text{ (deg.)} & \text{Saddle} \end{cases}$$
(3)

The parameters used in Eq. (3) are defined in Fig. 3. As an example, the weld profile generated for a sample joint model ( $\beta = 0.3$ ,  $\gamma = 12$ ,  $\tau = 0.4$ ,  $\alpha = 16$ ) is shown in Fig. 4. For details of the weld profile modeling according to AWS D 1.1 (2002) specifications, the reader is referred to Lie *et al.* (2001) and Ahmadi *et al.* (2012).

#### 3.2 Simulation of the steel-concrete interaction

A contact pair was defined at the interface between the steel chord member and the concrete inside it. The interaction between the outer surface of the concrete and the inner surface of the chord was considered to be due to friction only. A flexible and standard frictional contact of the surface-to-surface type was modeled in ABAQUS. The finite sliding feature was implemented due to the relatively large displacement between the contact surfaces, especially under the tensile loading condition. The concrete surface was defined as the main surface and the inner surface of the chord was introduced as the secondary surface. Separation between the two contact surfaces was permitted, with no shrinkage gap included. The penetration of one surface into the other was not allowed.

The coefficient of friction between concrete and steel depends on factors like surface roughness, contact conditions (dry or lubricated), and load history. For engineering purposes, commonly cited values are 0.3–0.4 for dry and smooth surfaces. To determine an appropriate coefficient of friction, a range of values between 0.25 and 0.4 was tested in the simulation, and a friction coefficient of

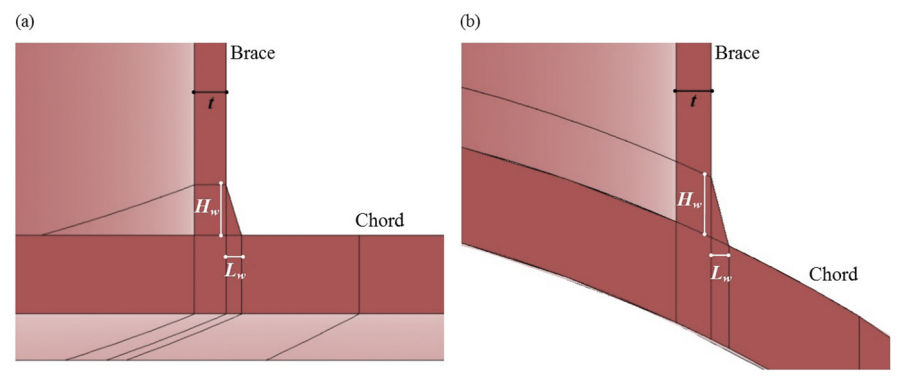


Fig. 3 Weld dimensions: (a) Crown position and (b) Saddle position

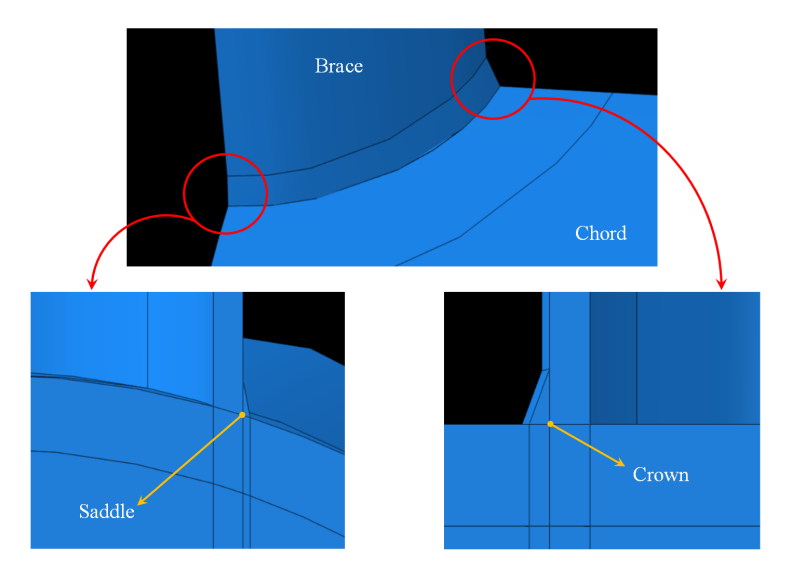


Fig. 4 The weld profile generated for a sample T-joint model ( $\beta = 0.3$ ,  $\gamma = 12$ ,  $\tau = 0.4$ ,  $\alpha = 16$ )

0.35 was chosen, as it provided the best correlation with the results from the verification model and was within the commonly cited values. The bonding between the concrete and the chord was neglected, as it is anticipated to deteriorate after a few loading cycles.

For additional information on the modeling of contact in FE software packages, the reader is referred to Nassiraei (2019, 2024a, b).

# 3.3 Load application and boundary conditions

As shown in Fig. 1(c), two types of axial loading were covered in the FE analysis. In offshore structures, the chord end fixity conditions of tubular joints may range from almost fixed to almost pinned with generally being closer to almost fixed (Efthymiou 1988). In practice, the value of the parameter  $\alpha$  in over 60% of tubular joints is in excess of 20 and is bigger than 40 in 35% of the

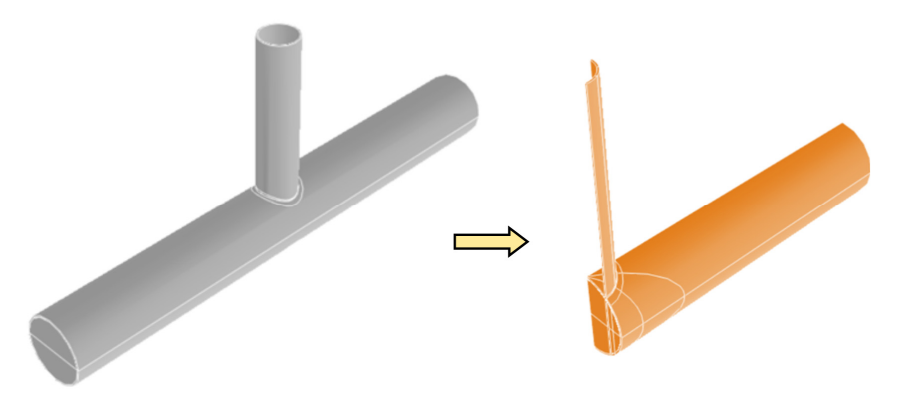


Fig. 5 One fourth of the entire tubular T-joint with concrete-filled chord required to be modeled under axial loading conditions

joints (Smedley and Fisher 1991). Changing the end restraint from fixed to pinned results in a maximum increase of 15% in the SCF at the crown position for joints with  $\alpha = 6$ , and this increase reduces to only 8% for  $\alpha = 8$  (Morgan and Lee 1998). In the view of the fact that the effect of chord end restraints is only significant for joints with  $\alpha < 8$  and high  $\beta$  and  $\gamma$  values, which do not commonly occur in practice, both chord ends were assumed to be fixed, with the corresponding nodes restrained. Due to the symmetry in geometry and loading of the joint, only  $\frac{1}{4}$  of the entire tubular T-joint with concrete-filled chord is required to be modeled in order to reduce the computational time (Fig. 5). Appropriate symmetric boundary conditions were defined for the nodes located on the symmetry planes.

# 3.4 Mesh generation

In the present study, C3D8I 3D elements were used to model the steel chord, steel brace, and weld profile. This ABAQUS element type is well-suited to model curved boundaries; and using this type of 3D solid elements, the weld profile can be modeled as a sharp notch. The C3D8I 3D is a linear hexahedral element defined by 8 nodes having three degrees of freedom per node and may have any spatial orientation. C3D8R 3D solid elements were used to mesh the concrete part of the model inside the chord. This mesh generation approach based on solid elements produces more accurate and detailed stress distribution near the brace-to-chord intersection in comparison with a shell analysis.

The mesh compatibility at the interface between the steel and concrete parts of the model is crucial for obtaining accurate results. Extreme care was taken during the mesh generation to ensure that the concrete and steel nodes coincide with each other at the interface. To guarantee the mesh quality, a sub-zone mesh generation scheme was used during the FE modeling. The entire structure was divided into several zones according to computational requirements. The mesh of each zone was generated separately and then the mesh of the entire joint was produced by merging the meshes of all the sub-zones. This scheme can feasibly control the mesh quantity and quality and avoid badly distorted elements. The mesh generated by this procedure for a tubular T-joint with concrete-filled chord is shown in Fig. 6.

It is explained in Sect. 3.5 that geometric stresses perpendicular to the weld toe are required to

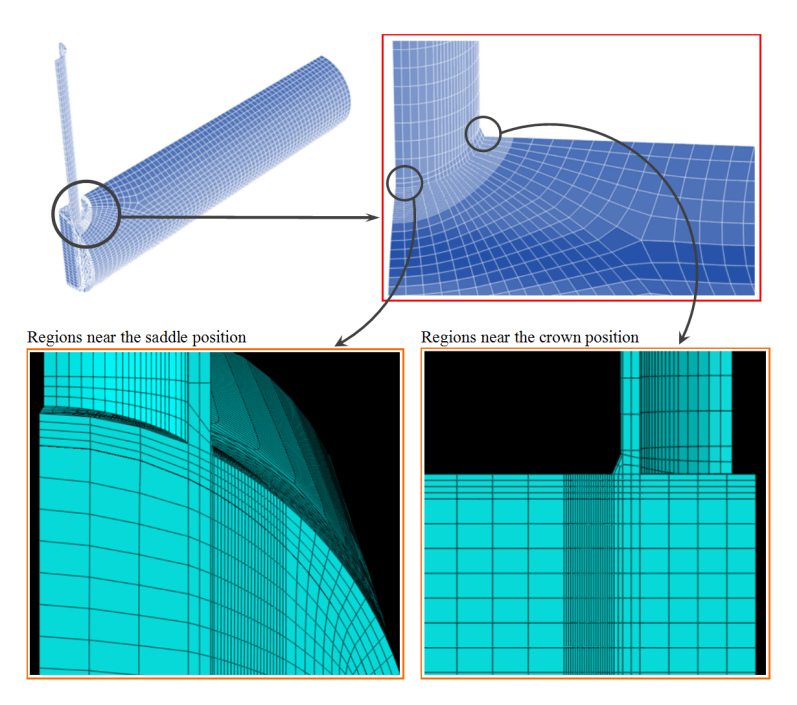


Fig. 6 Generated mesh by the sub-zone scheme

be calculated in order to determine the DoB at the weld toe position based on Eq. (1). As shown in Fig. 6, to extract the geometric stresses perpendicular to the weld toe, the region near the weld toe was meshed finely. The width of this region is discussed in Sect. 3.5.

To make sure that the results of the FE analysis are not affected by the inadequate quality or the size of the generated mesh, convergence test was conducted and meshes with different densities were used in this test, before generating the 81 models. Based on the results of the convergence test, the number of elements through the thickness of the chord was 4, 3, and 2 for the  $\gamma$  values of 12, 18, and 24, respectively; and as can be seen in Fig. 6, the number of elements through the thickness of the brace member was 2. The number of elements along ¼ of brace-chord intersection was 21. The number of elements on the surface, base, and back of the weld profile was 2; and the number of elements inside the extrapolation region was 22.

#### 3.5 Analysis procedure and extraction of DoB values

To determine the DoB values in a tubular joint, static analysis of the linearly elastic type is suitable (Ahmadi and Amini Niaki 2019). The Young's modulus and Poisson's ratio of steel were taken to be 210 GPa and 0.3, respectively. These material properties were assumed to be 30 GPa and 0.2 for concrete, respectively. Deformed shapes of the model subjected to compression and tension at crown and saddle positions are shown in Fig. 7 for a sample joint ( $\beta = 0.3$ ,  $\gamma = 12$ ,  $\tau =$  $0.7, \alpha = 16$ ).

To obtain the weld-toe DoB values, according to Eq. (1), bending and membrane stress components should be known. These components can be calculated as follows

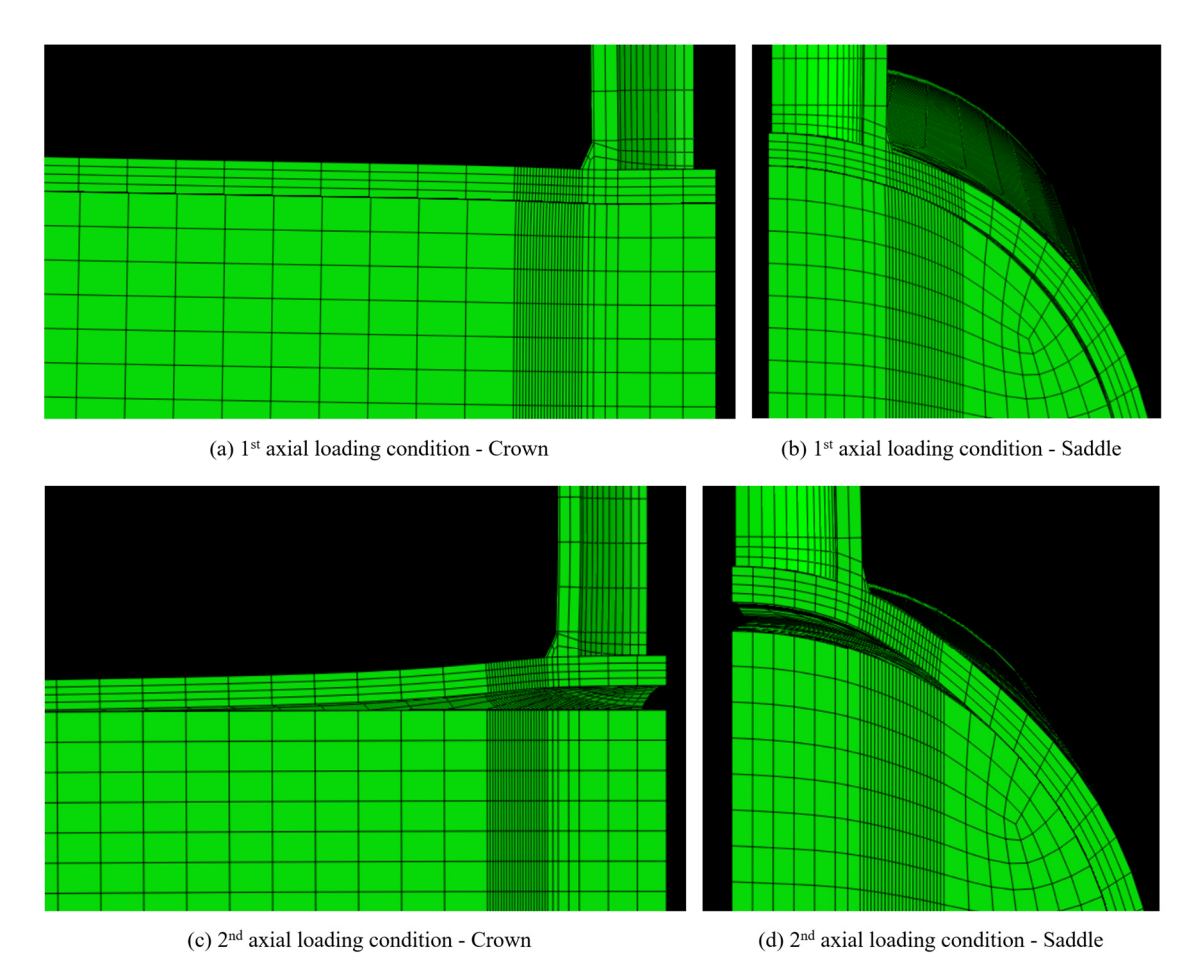


Fig. 7 Deformed shapes of the model subjected to compression and tension at crown and saddle positions ( $\beta = 0.3$ ,  $\gamma = 12$ ,  $\tau = 0.7$ ,  $\alpha = 16$ )

$$\sigma_B = \frac{\sigma_O - \sigma_I}{2} \tag{4}$$

$$\sigma_M = \frac{\sigma_O + \sigma_I}{2} \tag{5}$$

In Eqs. (4) and (5),  $\sigma_0$  and  $\sigma_1$  are HSS values at the weld toe on the outer and inner surfaces of the chord, respectively. The combination of Eqs. (1), (4) and (5) leads to the following equation

$$DoB = \frac{1}{2} \left( 1 - \frac{\sigma_I}{\sigma_O} \right) \tag{6}$$

To determine the HSS values, the stress at the weld-toe position should be extracted from the stress field outside the region influenced by the local weld-toe geometry. The location from which the stresses have to be extrapolated, called the extrapolation region (Fig. 8(a)), depends on the

Table 1 Boundaries of the extrapolation region recommended by CIDECT Design Guide (Zhao et al. 2001)

Distance from weld toe	Crown position on the chord side	Saddle position on the chord side
$l_{r.\mathrm{min}}{}^1$	0.4T	0.4T
$l_{r.{ m max}}{}^2$	$0.4\sqrt[4]{rtRT}$	0.09 <i>R</i>

<sup>&</sup>lt;sup>1</sup> Minimum value of  $l_{r,min}$ : 4 mm

<sup>&</sup>lt;sup>2</sup> Minimum value of  $l_{r,\text{max}}$ :  $l_{r,\text{min}} + 0.6t$ 

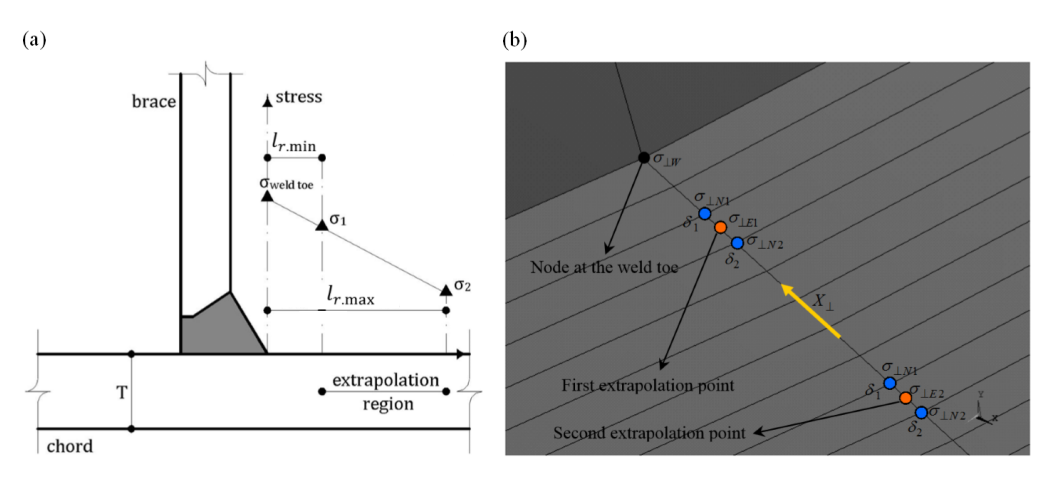


Fig. 8 (a) Extrapolation method according to CIDECT Design Guide (Zhao et al., 2001) and (b) Required interpolations and extrapolations to extract the HSS value at the weld toe

dimensions of the joint and the position along the intersection. Locations of the first and second extrapolation points selected according to the recommendations of CIDECT Design Guide (Zhao et al. 2001) are summarized in Table 1.

To extract and extrapolate the stresses perpendicular to the weld toe, as shown in Fig. 8(b), the region between the weld toe and the second extrapolation point was meshed in such a way that each extrapolation point was placed between two nodes located in its immediate vicinity. These nodes are located on the element-generated lines which are perpendicular to the weld toe ( $X_{\perp}$ direction in Fig. 8(b)).

At an arbitrary node inside the extrapolation region, the stress component in the direction perpendicular to the weld toe can be calculated, through the transformation of primary stresses in the global coordinate system, using the following equation

$$\sigma_{\perp N} = \sigma_x l_1^2 + \sigma_y m_1^2 + \sigma_z n_1^2 + 2(\tau_{xy} l_1 m_1 + \tau_{yz} m_1 n_1 + \tau_{zx} n_1 l_1)$$
(7)

where  $\sigma_a$  and  $\tau_{ab}(a, b = x, y, z)$  are components of the stress tensor which can be extracted from ABAQUS analysis results; and  $l_1$ ,  $m_1$ , and  $n_1$  are transformation components.

At the saddle and crown positions, Eq. (7)) is simplified as

$$\sigma_{\perp N} = \sigma_y m_1^2 + \sigma_z n_1^2 + 2\tau_{yz} m_1 n_1 \quad \text{(Saddle)} ; \quad \sigma_{\perp N} = \sigma_x \quad \text{(Crown)}$$

Transformation components can be obtained as follows

Table 2 Values assigned to  $c_1$  and  $c_2$  coefficients in Eq. (12) at crown and saddle positions

Geo	ometrical paran	neters	Cro	own	Sac	ldle
β	γ	τ	$c_1$	$c_2$	$c_1$	$c_2$
0.3	12	0.4	1.96165	0.96165	1.5882	0.5882
0.3	12	0.7	1.74348	0.74348	1.5882	0.5882
0.3	12	1	1.63951	0.63951	1.5882	0.5882
0.3	18	0.4	1.66794	0.66794	1.32786	0.32786
0.3	18	0.7	1.53416	0.53416	1.32786	0.32786
0.3	18	1	1.46731	0.46731	1.32786	0.32786
0.3	24	0.4	1.53096	0.53096	1.22727	0.22727
0.3	24	0.7	1.43172	0.43172	1.22727	0.22727
0.3	24	1	1.38085	0.38085	1.22727	0.22727
0.45	12	0.4	1.79595	0.79595	1.5882	0.5882
0.45	12	0.7	1.62687	0.62687	1.5882	0.5882
0.45	12	1	1.54428	0.54428	1.5882	0.5882
0.45	18	0.4	1.56704	0.56704	1.32786	0.32786
0.45	18	0.7	1.45904	0.45904	1.32786	0.32786
0.45	18	1	1.40405	0.40405	1.32786	0.32786
0.45	24	0.4	1.4564	0.4564	1.22727	0.22727
0.45	24	0.7	1.37452	0.37452	1.22727	0.22727
0.45	24	1	1.33194	0.33194	1.22727	0.22727
0.6	12	0.4	1.70195	0.70195	1.5882	0.5882
0.6	12	0.7	1.55907	0.55907	1.5882	0.5882
0.6	12	1	1.48808	0.48808	1.5882	0.5882
0.6	18	0.4	1.50775	0.50775	1.32786	0.32786
0.6	18	0.7	1.41399	0.41399	1.32786	0.32786
0.6	18	1	1.36577	0.36577	1.32786	0.32786
0.6	24	0.4	1.41171	0.41171	1.22727	0.22727
0.6	24	0.7	1.33968	0.33968	1.22727	0.22727
0.6	24	1	1.30196	0.30196	1.22727	0.22727

$$m_1 = \cos(X_{\perp}, y) = (y_w - y_n)/\delta$$
;  $n_1 = \cos(X_{\perp}, z) = (z_w - z_n)/\delta$  (9)

$$\delta = \sqrt{(x_w - x_n)^2 + (y_w - y_n)^2 + (z_w - z_n)^2}$$
 (10)

where  $X_{\perp}$  is the direction perpendicular to the weld toe (Fig. 7(b)); x, y, and z are the axes of global Cartesian coordinate system;  $(x_n, y_n, z_n)$  and  $(x_w, y_w, z_w)$  are coordinates of the considered node inside the extrapolation region and its corresponding node at the weld toe position, respectively; and  $\delta$  is the distance between the weld toe and the considered node inside the extrapolation region.

Stress at an extrapolation point is obtained as follows

$$\sigma_{\perp E} = \frac{\sigma_{\perp N1} - \sigma_{\perp N2}}{\delta_1 - \delta_2} (\Delta - \delta_2) + \sigma_{\perp N2}$$
(11)

where  $\sigma_{\perp Ni}$  (i = 1 and 2) is the nodal stress in the immediate vicinity of the extrapolation point in a

direction perpendicular to the weld toe (Eq. (8));  $\delta_i$  (i = 1 and 2) is obtained by Eq. (10).

At both saddle and crown positions, the value of  $\Delta$  equals to 0.4T for the first extrapolation points. For the second extrapolation point, the value of  $\Delta$  equals to 0.09R and  $0.4\sqrt[4]{rtRT}$  at saddle and crown positions, respectively (Fig. 8(b)).

The extrapolated stress at the weld toe position, HSS, is calculated by the following equation

$$\sigma_{\perp W} = c_1 \sigma_{\perp E1} - c_2 \sigma_{\perp E2} \tag{12}$$

where  $\sigma_{\perp E1}$  and  $\sigma_{\perp E2}$  are the stresses at the first and second extrapolation points in the direction perpendicular to the weld toe, respectively (Eq. (11)), and  $c_1$  and  $c_2$  are geometry-dependent coefficients listed in Table 2.

If the considered nodes in the calculations of Eqs. (8)-(12) are located on the outer surface of the chord, the value of  $\sigma_{\perp W}$  obtained from Eq. (12) is used as  $\sigma_0$  in Eq. (6); and if the considered nodes are located on the inner surface of the chord, the result of Eq. (12) is equivalent to  $\sigma_I$  which is required for the calculation of the DoB in Eq. (6).

#### 3.6 FE model verification

As far as the authors are aware, there is no experimental/numerical data available in the literature on the DoB values in tubular T-joints with concrete-filled chords. However, previous research works offer some experimental data and parametric equations that can be used to validate the FE models developed in the present study.

# 3.6.1 Comparison with experimental data for the HSS

According to Eq. (6), DoB is a function of  $\sigma_0$  and  $\sigma_I$  that are the HSS values at the weld toe on the outer and inner surfaces of the chord, respectively. Hence, if the proposed FE model could

Table 3 Geometrical properties of the tubular T-joint with and without the concrete fill used for the verification of FE models based on available experimental data and parametric equations

Parameter	D (mm)	T (mm)	L (mm)	d (mm)	t (mm)	l (mm)	τ	β	γ	α	$\alpha_B$
Value	165.10	5.32	1200	48.3	5.27	570	0.99	0.29	15.5	14.53	23.6

Table 4 Results of the FE model verification based on available experimental data

Dogition		HSS	— Difference
Position —	Present FE model	Musa et al. (2018) test	— Difference
Crown	4.69	5.34	12.58%

Table 5 Results of the FE model verification based on available parametric equations

Position	DoB			
Fosition	Present FE model	Chang and Dover (1999) equations	— Difference	
Saddle	0.748	0.872 {from Eq. (A7) of Chang and Dover (1999)}	15.30%	

Parameter	Definition	Value(s)
β	d/D	0.3, 0.45, 0.6
γ	D/2T	12, 18, 24
τ	t/T	0.4, 0.7, 1.0
$\alpha$	2L/D	8, 16, 24
Øp.	21/d	8

Table 6 Values assigned to each dimensionless parameter

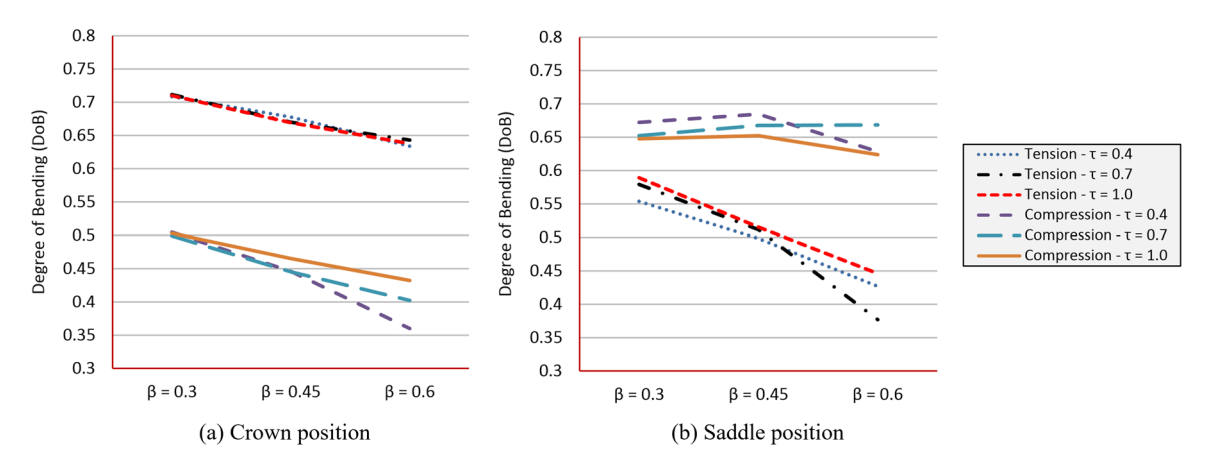


Fig. 9 Effects of the  $\beta$  on DoB values and its interaction with the  $\tau$  ( $\gamma = 12$ ,  $\alpha = 24$ )

the HSS accurately, then undoubtedly it is capable of resulting in accurate DoB values. To verify the developed FE modeling procedure, a validating FE model was generated, and its results were compared with the results of experimental tests conducted by Musa *et al.* (2018) on T-joints with concrete-filled chords. Geometrical properties of validating FE model are listed in Table 3 and results of the verification process are presented in Table 4. It can be seen that there is a good agreement between the results of the present FE model and experimental data. Hence, the developed FE model can be considered to be accurate enough to provide valid results.

#### 3.6.2 Comparison with available DoB parametric equations

A set of parametric equations developed by Chang and Dover (1999) for the prediction of DoB values in axially loaded tubular T-joints without the concrete fill was used in the present study to validate the generated FE models. A validating FE model was generated for an unreinforced T-joint with typical geometrical characteristics (Table 3) and the model was analyzed subjected to axial loading. Results of the verification process presented in Table 5 indicate that there is a good agreement between the results of unreinforced FE model and equations proposed by Chang and Dover (1999) which lends some support to the validity of DoB values derived from the concrete-filled joint FE models.

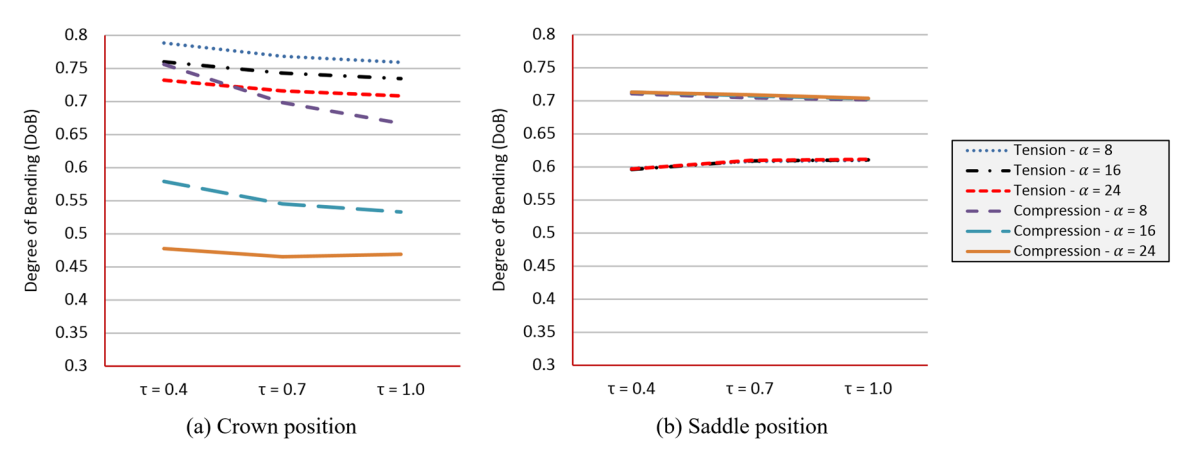


Fig. 10 Effects of the  $\tau$  on DoB values and its interaction with the  $\alpha$  ( $\gamma = 18, \beta = 0.45$ )

## 4. Effects of geometrical parameters, loading type, and concrete fill on DoB values

## 4.1 Parametric study

In order to study the DoB in tubular T-joints with concrete-filled chords subjected to two types of axial loading (Fig. 1(c)), 162 stress analyses were conducted on 81 FE models using ABAQUS. The objective was to investigate the effects of dimensionless geometrical parameters on the DoB values at saddle and crown positions. Different values assigned to parameters  $\beta$ ,  $\gamma$ ,  $\tau$ , and  $\alpha$  are listed in Table 6. These values cover the practical ranges of dimensionless parameters typically found in tubular joints of offshore jacket structures. The brace length has no effect on the HSS values when the parameter  $\alpha_B$  is greater than a critical value (Chang and Dover 1999). According to Chang and Dover (1996), this critical value is about 6. In the present study, to avoid the effect of short brace length, a realistic value of  $\alpha_B = 8$  was assigned to all joints. The 81 generated models span the following ranges of dimensionless geometrical parameters

$$0.3 \le \beta \le 0.5$$
 $12 \le \gamma \le 24$ 
 $0.4 \le \tau \le 1.0$ 
 $8 \le \alpha \le 24$ 
(13)

#### 4.2 Effects of the $\beta$ , $\tau$ , $\gamma$ , and $\alpha$

The parameter  $\beta$  is the ratio of brace diameter to chord diameter. Hence, the increase of the  $\beta$  in models having constant value of chord diameter results in an increase of brace diameter. Fig. 9, as an example, depicts the change of values at crown and saddle positions due to the change in the value of the  $\beta$  and the interaction of this parameter with the  $\tau$ . In this study, the influence of parameters  $\gamma$  and  $\alpha$  over the effect of the  $\beta$  on the DoB was also investigated. A large number of comparative charts were used to study the effect of t DoB he  $\beta$  and only two of them are presented

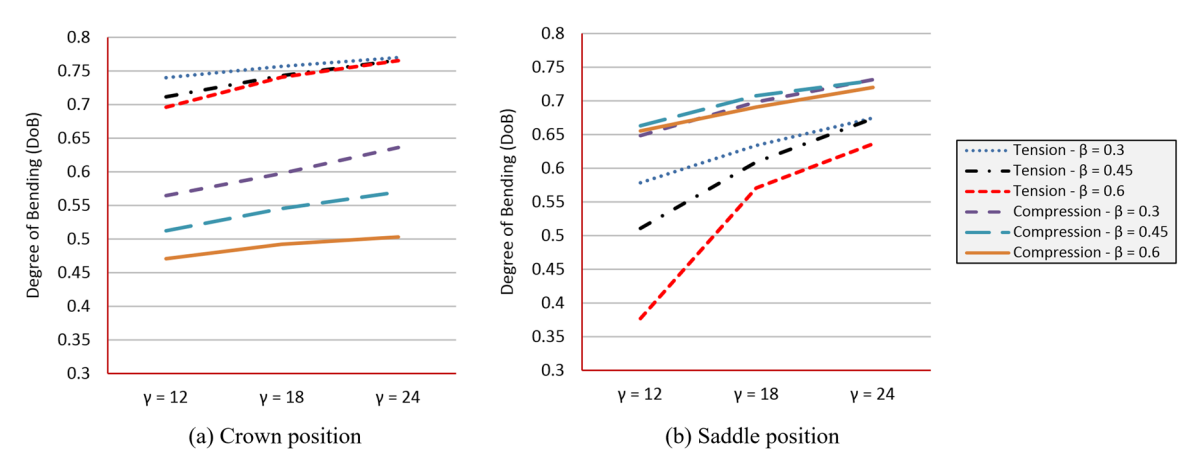


Fig. 11 Effects of the  $\gamma$  on DoB values and its interaction with the  $\beta$  ( $\tau = 0.7$ ,  $\alpha = 16$ )

in Fig. 9 for the sake of brevity. Results showed that the increase of the  $\beta$  generally results in a decrease of DoB values at the crown position (Fig. 9(a)). This conclusion is not dependent on the values of other geometrical parameters. At the saddle position, the effect of the  $\beta$  on DoB values depends on the axial loading type. Subjected to tension, the increase of the  $\beta$  leads to a decrease of the DoB at the saddle position; while subjected to compression, a regular pattern cannot be identified, and the amount of change is generally not significant (Fig. 9(b)).

The parameter  $\tau$  is the ratio of brace thickness to chord thickness and the  $\gamma$  is the ratio of radius to thickness of the chord. Hence, the increase of the  $\tau$  in models having constant value of the  $\gamma$  results in the increase of the brace thickness. For example, Fig. 10 shows the change of DoB values at crown and saddle positions due to the change of the  $\tau$  and the interaction of this parameter with the  $\alpha$ . In this study, the interaction of the  $\tau$  with the other geometrical parameters was also investigated. Results indicated that the increase of the  $\tau$  leads to a decrease of the DoB at the crown position (Fig. 10(a)) However, the amount of change is usually small. At the saddle position, the effect of the  $\tau$  on DoB values depends on the axial loading type. Subjected to tension, the increase of the  $\tau$  leads to the decrease of the DoB at the saddle position; while subjected to compression, the increase of the parameter  $\tau$  results in the increase of the DoB at the saddle position. It should also be noted that the amount of DoB variation at the saddle position due to the change of the  $\tau$  is generally insignificant (Fig. 10(b))

The parameter  $\gamma$  is the ratio of the radius to the thickness of the chord. Hence, the increase of the  $\gamma$  in models having constant value of the chord diameter means the decrease of chord thickness. Two charts are presented in Fig. 11, as an example, depicting the change of the DoB at crown and saddle positions due to the change in the value of the  $\gamma$  and the interaction of this parameter with the  $\beta$ . In this study, the influence of parameters  $\tau$  and  $\alpha$  over the effect of the  $\gamma$  on DoB values was also investigated. It was observed that the increase of the  $\gamma$  leads to the increase of the DoB at both crown and saddle positions. It can also be seen that the greatest changes in the DoB due to the change of the  $\gamma$  occur at the saddle position and subjected to tension.

The parameter  $\alpha$  is the ratio of the length to the radius of the chord. Hence, the increase of the  $\alpha$  in models having constant value of the chord diameter means the increase of the chord length. For example, Fig. 12 shows the change of DoB values at crown and saddle positions due to the change

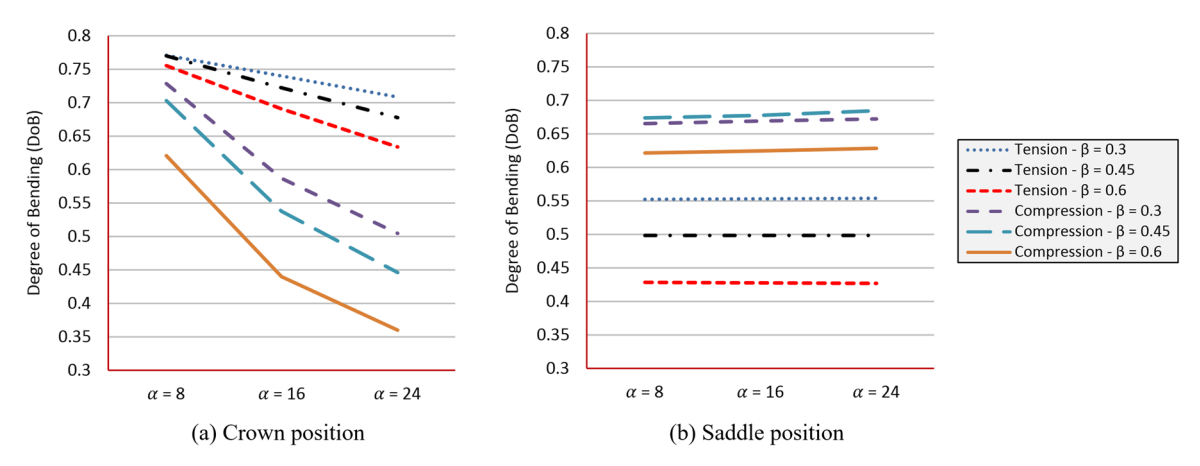


Fig. 12 Effects of the  $\alpha$  on DoB values and its interaction with the  $\beta$  ( $\tau = 0.4$ ,  $\gamma = 12$ )

in the value of the  $\alpha$  and the interaction of this parameter with the  $\beta$ . In this study, the interaction of the  $\alpha$  with the other geometrical parameters was also investigated. Results showed that the increase of the  $\alpha$  generally leads to the decrease of the DoB at the crown position; but it does not have a considerable effect on the DoB values at the saddle position. It can also be seen that at the crown position, the amount of DoB change due to the change of the  $\alpha$  subjected to compression is more significant compared to tension.

#### 4.3 Remarks on low DoB and effects of position and loading type

Figs. 9-12 indicate that DoB values smaller than 0.8 have been frequently observed in axially loaded tubular T-joints with concrete-filled chords. The average DoB values for the 81 studied joint models at crown and saddle positions subjected to the 1st axial loading condition (brace compression) are 0.571 and 0.691, respectively. For the 2<sup>nd</sup> axial loading condition (brace tension), the average DoB values are 0.742 and 0.587 at crown and saddle positions, respectively.

As mentioned earlier, typical DoB values are in the range of 0.8-0.9 for the joints used to derive the S-N curves; and smaller values can be considered as low DoB (Chang and Dover 1999). Hence, it is quite common for an axially loaded tubular T-joint with concrete-filled chord to have a low DoB. As previously discussed, Eide et al. (1993) has confirmed the detrimental effect of low DoB on fatigue life. Therefore, when the current standard HSS-based S-N approach is used for the fatigue analysis of axially loaded tubular T-joints with concrete-filled chords, results should be modified to include the effect of the DoB to obtain a more accurate fatigue life prediction.

Results obtained from the 162 stress analyses conducted on developed FE models indicate that, on an average basis, the DoB values at saddle and crown positions subjected to brace compression and tension can be ranked as follows.

$$DoB_{1C} < DoB_{2S} < DoB_{1S} < DoB_{2C}$$
 (14)

where DoB<sub>1C</sub> and DoB<sub>2C</sub> denote the DoB values at the crown position subjected to the 1<sup>st</sup> and  $2^{nd}$  axial loading conditions, respectively; and  $DoB_{1S}$  and  $DoB_{2S}$  refer to the DoB values at the saddle position subjected to the  $1^{st}$  and  $2^{nd}$  axial loading conditions, respectively.

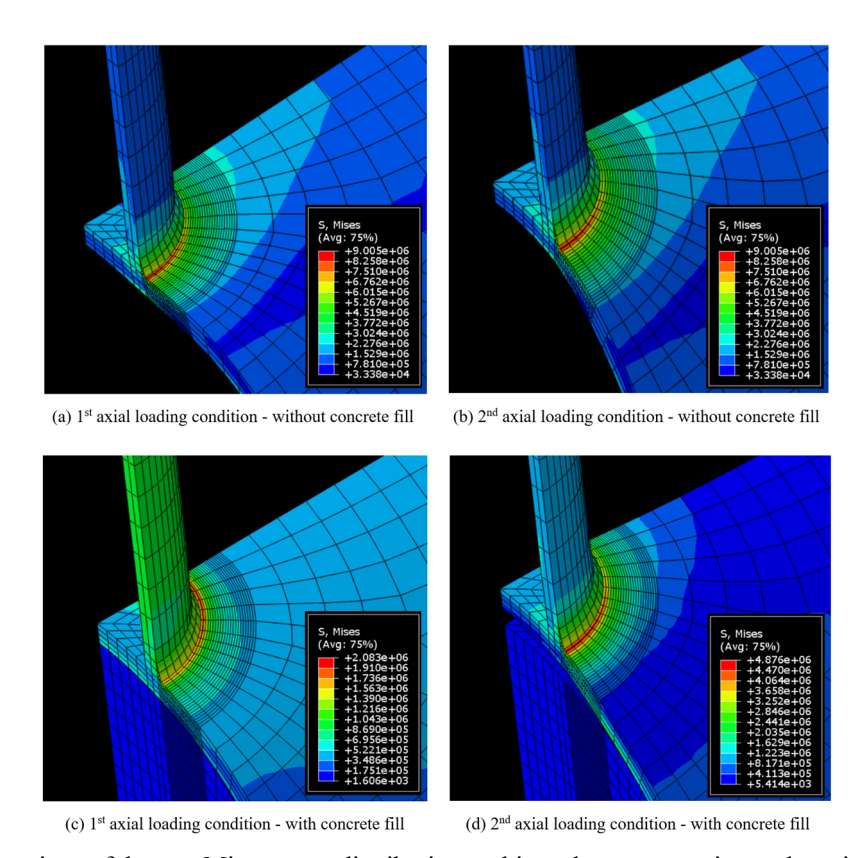


Fig. 13 Comparison of the von Mises stress distributions subjected to compression and tension in a sample tubular T-joint ( $\beta = 0.3$ ,  $\gamma = 12$ ,  $\tau = 0.7$ ,  $\alpha = 16$ ) with and without the chord concrete fill

## 4.4 Effect of concrete fill on the DoB values

Distributions of von Mises stresses in sample T-joints with and without the concrete fill in the chord member are compared in Fig. 13 for the tensile and compressive loads. It can be seen in Figs. 13(a) and 13(b) that in a tubular T-joint without the concrete fill, regardless of the type of brace axial loading (i.e. either tension or compression), the maximum stress always occurs at the saddle position which implies that the maximum HSS and SCF values also occur at the saddle position. It can also be seen that the values of the maximum von Mises stresses subjected to tension and compression are the same. However, as evidenced by Figs. 13(c) and 13(d) in a tubular T-joint with the concrete-filled chord, the maximum von Mises stresses subjected to compression and tension occur at the crown and saddle positions, respectively. This means that subjected to compression, the presence of concrete fill leads to shifting the position of the maximum HSS and SCF values from the saddle to the crown.

Comparing the maximum values of von Mises stress in T-joints with and without the chord concrete fill indicates that the presence of the concrete fill results in the reduction of von Mises stress subjected to both tensile and compressive axial loadings which means that the concrete fill reduces the HSS and SCF improving the fatigue life of the tubular joint. It can also be seen that subjected to a compressive load, the concrete fill is more effective in reducing the stress

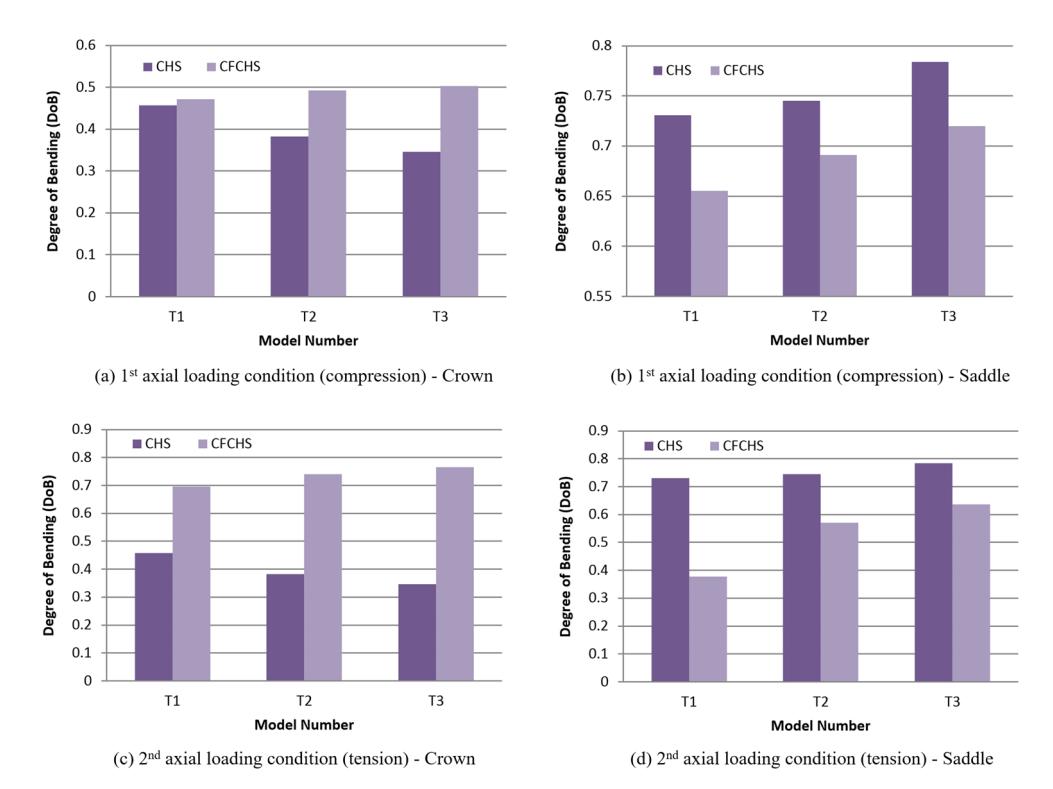


Fig. 14 Comparison of DoB values in three simple tubular T-joints (denoted by CHS) with the corresponding values in tubular T-joints with concrete-filled chords (denoted by CFCHS)

concentration compared to a tensile load. For instance, for the sample tubular T-joint shown in Fig. 13, the ratio of the maximum von Mises stress in the joint without the chord concrete fill to the corresponding stress in the joint with the chord concrete fill is 4.33 subjected to compressive load. This ratio for the tensile load is 1.85 which is less than half of the corresponding value subjected to compressive load.

Fig. 14 compares the DoB values in six sample tubular T-joints with and without the concrete fill in the chord member. Geometrical properties of the sample joints are given in Table 7. Fig. 14 indicates that there can be a quite big difference between the DoB values in tubular T-joints with and without the chord concrete fill. For example, subjected to the 2<sup>nd</sup> axial loading condition, the DoB value at the crown position of the CFCHS3 model is over twice the DoB value at the crown

Table 7 Geometrical properties of the six sample joints used to compare the DoB values in tubular T-joints with and without the concrete fill in the chord member

I-int ID	Geometrical properties						
Joint ID	D (mm)	τ	β	γ	α	$\alpha_B$	
T1 (CHS1 and CFCHS1)	500	0.7	0.6	12	16	8	
T2 (CHS2 and CFCHS2)	500	0.7	0.6	18	16	8	
T3 (CHS3 and CFCHS3)	500	0.7	0.6	24	16	8	

position of the corresponding CHS3 model (Fig. 14(c)); while, subjected to the same type of axial loading, the DoB value at the saddle position of the CFCHS1 model is approximately half of the DoB value at the saddle position of the corresponding CHS1 model (Fig. 14(d)).

Fig. 14 also shows that, regardless of the brace axial loading type (i.e., either compression or tension), the DoB values at the crown position of concrete-filled joints are always larger than the corresponding values for the simple joints without the chord concrete fill. On the contrary, at the saddle position, the DoB values for the joints with concrete-filled chords are smaller than the corresponding DoB values obtained from the simple T-joints without the chord concrete fill.

The above discussion implies that the positive or negative effect of concrete fill on fatigue life can only be judged on a case-by-case basis because it depends on the relative amount of increase/decrease of SCF and DoB at saddle and crown positions. However, since the effect of SCF on fatigue life is generally more pronounced compared to DoB, it is expected that, in most cases, the presence of concrete fill will result in the improvement of fatigue life.

It can be concluded from Fig. 14 that for axially loaded T-joints with concrete-filled chords, the parametric formulas of simple T-joints are not applicable for the DoB prediction, since such formulas may lead to under-/over-predicting results. Consequently, developing a set of specific parametric equations for the DoB calculation in tubular T-joints with concrete-filled chords has practical value for design purposes.

# 5. Deriving parametric equations for the DoB calculation

Four individual parametric equations are proposed in the present paper, to calculate the DoB values at saddle and crown positions on the weld toe of tubular T-joints with concrete-filled chords subjected to two types of axial loading (Fig. 1(c)). Results of multiple nonlinear regression analyses performed by SPSS were used to develop these parametric DoB formulas. Values of dependent variable (i.e., DoB) and independent variables (i.e.  $\beta$ ,  $\gamma$ ,  $\tau$ , and  $\alpha$ ) constitute the input data imported in the form of a matrix. Each row of this matrix involves information about the DoB value at a considered position on the chord-side weld toe of a tubular T-joint with concrete-filled chord having specific geometrical properties.

When the dependent and independent variables are defined, a model expression must be built with defined parameters. Parameters of the model expression are unknown coefficients and exponents. The researcher must specify a starting value for each parameter, preferably as close as possible to the expected final solution. Poor starting values can result in failure to converge or in convergence on a solution that is local (rather than global) or is physically impossible. Various model expressions must be built to derive a parametric equation having a high coefficient of determination ( $R^2$ ).

Following parametric equations are proposed, after performing a large number of nonlinear analyses, for the calculation of DoB values at saddle and crown positions in tubular T-joints with concrete-filled chords subjected to two types of axial loading (Fig. 1(c)).

1<sup>st</sup> axial loading condition (brace compression)

Crown: DoB = 
$$0.756\beta^{-0.246}\gamma^{0.142}\tau^{-0.073}\alpha^{-0.35}$$
  $R^2 = 0.946$  (15)

Saddle: DoB = 
$$-1.074\beta^{0.084}\gamma^{-0.476}\tau^{0.088}\alpha^{-0.022} + 0.928$$
  $R^2 = 0.894$  (16)

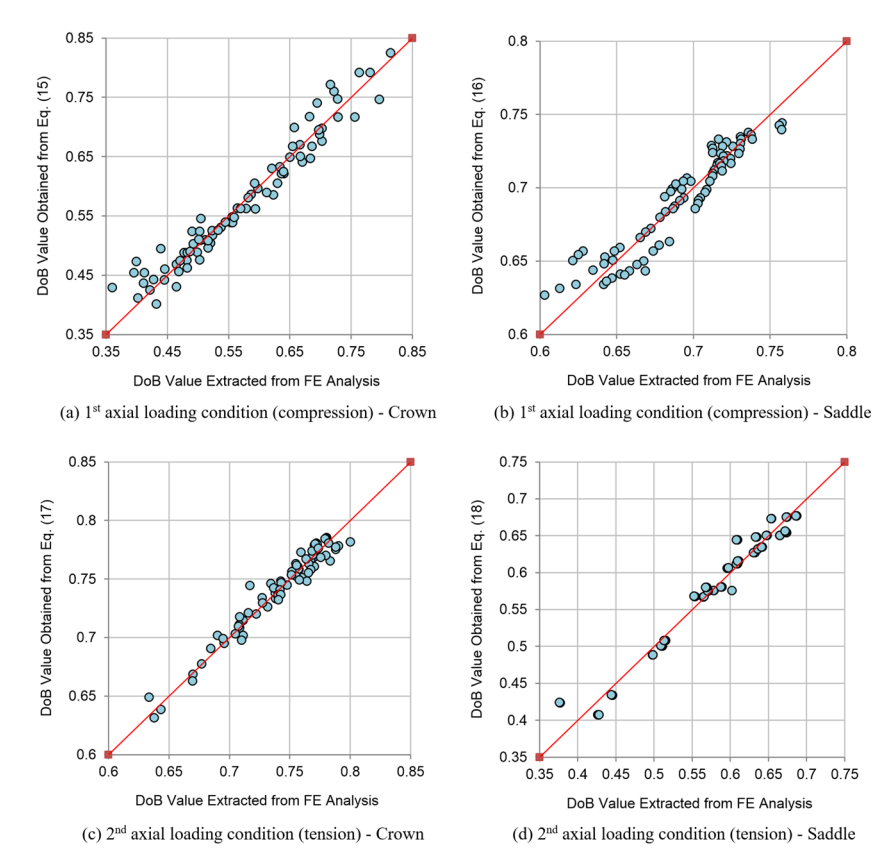


Fig. 15 Comparison of 81 DoB values calculated by the proposed equations with the corresponding DoB values extracted from the FE analysis

Table 8 Confidence interval of parameter estimates for the DoB equation proposed for the crown position under axial compression (Eq. (15))

D	Estimata	95% confidence interval				
Parameter	Estimate –	Lower bound	Upper bound			
$a_1$	0.756	0.729	0.783			
$a_2$	-0.246	-0.340	-0.152			
$a_3$	0.142	0.106	0.178			
$a_4$	-0.073	-0.095	-0.051			
$a_5$	-0.350	-0.387	-0.314			

2nd axial loading condition (brace tension)

Crown: DoB = 
$$-0.187\beta^{0.744}\gamma^{-1.306}\tau^{0.124}\alpha^{1.101} + 0.796$$
  $R^2 = 0.953$  (17)

Saddle: DoB = 
$$-43.131\beta^{1.063}\gamma^{-1.808}\tau^{-0.099}\alpha^{0.001} + 0.715$$
  $R^2 = 0.961$  (18)

Values obtained for  $R^2$ , indicating the accuracy of the fit, are considered to be acceptable regarding the complex nature of the problem.

In order to give an insight into the uncertainty involved in estimating the parameters, 95% confidence intervals of the estimates are presented in Tables 8-11 for Eqs. (15)-(18), respectively.

Such confidence interval for a parameter estimate is a range that includes it with the probability of 95%. Correlations of parameter estimates are presented in Tables 12-15. The ranges of dimensionless geometrical parameters for the developed equations are given in Eq. (13). Proposed equations may not be valid outside the ranges indicated in Eq. (13).

Table 9 Confidence interval of parameter estimates for the DoB equation proposed for the saddle position under axial compression (Eq. (16))

Danamatan	Datingete	95% confidence interval			
Parameter	Estimate –	Lower bound	Upper bound		
$a_1$	-1.074	-1.820	-0.328		
$a_2$	0.084	-0.576	0.744		
$a_3$	-0.476	-0.598	-0.355		
$a_4$	0.088	0.049	0.127		
$a_5$	-0.022	-0.147	0.103		
$a_6$	0.928	0.598	1.258		

Table 10 Confidence interval of parameter estimates for the DoB equation proposed for the crown position under axial tension (Eq. (17))

D	F-4:4-	95% confidence interval				
Parameter	Estimate –	Lower bound	Upper bound			
$a_1$	-0.187	268	-0.106			
$a_2$	0.744	0.599	0.888			
$a_3$	-1.306	-1.517	-1.095			
$a_4$	0.124	0.047	0.200			
$a_5$	1.101	0.900	1.301			
$a_6$	0.796	0.787	0.805			

It should also be noted that the developed equations are only valid for axial loading and the application of proposed equations for in-plane and out-of-plane bending loadings may lead to significantly inaccurate results.

In Fig. 15, the DoB values predicted by proposed equations are compared with the DoB values extracted from FE analyses. It can be seen that there is a good agreement between the results of proposed equations and numerically computed values.

Table 11 Confidence interval of parameter estimates for the DoB equation proposed for the saddle position under axial tension (Eq. (18))

D	Estimata	95% confidence interval				
Parameter	Estimate –	Lower bound	Upper bound			
$a_1$	-43.131	-81.504	-4.757			
$a_2$	1.063	0.866	1.260			
$a_3$	-1.808	-2.155	-1.461			
$a_4$	-0.099	-0.164	-0.033			
$a_5$	0.001	-0.052	0.055			
$a_6$	0.715	0.690	0.739			

 $DoB = a_1 \beta^{a_2} \gamma^{a_3} \tau^{a_4} \alpha^{a_5} + a_6$ 

Table 12 Correlations of parameter estimates for the DoB equation of the crown position under compression (Eq. (15))

	$a_1$	$a_2$	$a_3$	$a_4$	$a_5$
$a_1$	1.000				
$a_2$	0.097	1.000			Symmetric
$a_3$	0.000	0.253	1.000		
$a_4$	0.000	-0.457	0.000	1.000	
$a_5$	0.000	-0.843	0.000	0.000	1.000

Table 13 Correlations of parameter estimates for the DoB equation of the saddle position under compression (Eq. (16))

· 1 ·	,,					
	$a_1$	$a_2$	$a_3$	$a_4$	$a_5$	$a_6$
$\overline{a_1}$	1.000					
$a_2$	0.989	1.000			Symmetric	
$a_3$	-0.941	-0.941	1.000			
$a_4$	0.810	0.760	-0.718	1.000		
$a_5$	-0.955	-0.967	0.914	-0.738	1.000	
$a_6$	0.981	0.998	-0.943	0.762	-0.969	1.000

The UK Department of Energy (1983) recommends the following assessment criteria regarding the applicability of the parametric equations (P/R) stands for the ratio of the predicted DoB from a given equation to the recorded DoB from test or analysis):

- For a given dataset, if % DoB values under-predicting  $\leq 25\%$ , i.e.  $[\%P/R < 1.0] \leq 25\%$ , and if % DoB values considerably under-predicting  $\leq$  5%, i.e., [%P/R < 0.8]  $\leq$  5%, then accept the equation. If, in addition, the percentage DoB values considerably over-predicting  $\leq$  50%, i.e. [%P/R > 1.5]  $\geq$  50%, then the equation is conservative.
- If the acceptance criteria is nearly met i.e.,  $25\% < [\%P/R < 1.0] \le 30\%$ , and/or 5% < [%P/R]< 0.8]  $\le 7.5\%$ , then the equation is regarded as borderline and engineering judgment must be used to determine acceptance or rejection.

• Otherwise reject the equation as it is too optimistic.

Since for a mean fit equation, there is a large percentage of under-prediction, the requirement for joint under-prediction, i.e., P/R < 1.0, can be removed in the assessment of parametric equations (Bomel Consulting Engineers 1994). Assessment results are presented in Table 16 showing that Eqs. (15)-(18) satisfy the UK DoE criteria in their present form and hence can reliably be used for the analysis and design of tubular T-joints with concrete-filled chords.

## 6. Application of DoB to improve the accuracy of fatigue life estimation

As mentioned earlier, there are two main approaches for the fatigue life estimation: stress-life (S-N) approach and fracture mechanics (FM) approach. In S-N approach, detrimental effect of low

Table 14 Correlations of parameter estimates for the DoB equation of the crown position under tension (Eq. (17))

	$a_1$	$a_2$	$a_3$	$a_4$	$a_5$	$a_6$
$a_1$	1.000					
$a_2$	0.014	1.000			Symmetric	
$a_3$	0.170	-0.558	1.000			
$a_4$	-0.021	0.128	-0.165	1.000		
$a_5$	0.515	0.580	-0.746	0.171	1.000	
$a_6$	-0.230	-0.659	0.847	-0.195	-0.880	1.000

Table 15 Correlations of parameter estimates for the DoB equation of the saddle position under tension (Eq. (18))

• //						
	$a_1$	$a_2$	$a_3$	$a_4$	$a_5$	$a_6$
$a_1$	1.000					
$a_2$	-0.831	1.000			Symmetric	
$a_3$	0.983	-0.807	1.000			
$a_4$	0.162	-0.179	0.198	1.000		
$a_5$	0.157	0.003	-0.003	-0.001	1.000	
$a_6$	0.925	-0.854	0.945	0.209	-0.004	1.000
<u>u</u> 6	0.723	0.054	0.773	0.207	0.004	1.,

Table 16 Results of DoB equations assessment according to the UK Department of Energy (1983) acceptance criteria

Axial loading type	Position	Equation -	Cond	- Decision	
Axiai loading type	Position		%P/R < 0.8	%P/R > 1.5	- Decision
1 <sup>st</sup> (Compression)	Crown	Eq. (15)	0.00% < 5% OK.	0.00% < 50% OK.	Accept
1 <sup>st</sup> (Compression)	Saddle	Eq. (16)	0.00% < 5 %  OK.	0.00% < 50% OK.	Accept
2 <sup>nd</sup> (Tension)	Crown	Eq. (17)	0.00% < 5% OK.	0.00% < 50% OK.	Accept
2 <sup>nd</sup> (Tension)	Saddle	Eq. (18)	0.00% < 5% OK.	0.00% < 50% OK.	Accept

DoB on fatigue life can be considered during the application of S-N curves. One option is to use the same modification format recommended by Sect. 5.5.2 of API RP 2A-WSD (2007) for considering the so-called thickness effect. i.e., if the joint's DoB is smaller than a critical value (e.g., 0.8), the number of stress cycles leading to the joint failure  $(N_0)$ , which has been obtained from a standard S-N curve, should be modified as follows

$$N = N_0 \left(\frac{\text{DoB}}{\text{DoB}_0}\right)^{\alpha} \tag{19}$$

where N is the modified number of stress cycles leading to the joint failure, DoB is the joint's degree of bending calculated by proposed equations (Eqs. (15)-(18)),  $DoB_0$  is the critical value (e.g., 0.8), and the power  $\alpha$  is a function of the joint geometry and quality of the weld that should be determined experimentally.

Fatigue life assessment based on FM approach involves calculating the number of stress cycles required for a given increase in crack size. This is implemented by assuming a suitable crack growth law such as the Paris equation. Using this technique, the number of stress cycles required to extend a fatigue crack from an initial depth  $a_i$  to any depth  $a_f$  is given as (Paris and Erdogan 1963)

$$N = \int_{a_i}^{a_f} \left( \frac{1}{C(\Delta K)^m} \right) da \tag{20}$$

where C and m are material constants, and  $\Delta K$  is the SIF range which expresses the effect of load range on the crack. It describes the stress field associated with the cracked body at the crack tip:

$$\Delta K = K_{\text{max}} - K_{\text{min}} = Y(a)\Delta\sigma\sqrt{\pi a}$$
(21)

where  $\Delta \sigma$  is the HSS range, a is the crack size, and Y is the modifying shape parameter that depends on the crack geometry and the geometry of the specimen.

The accurate determination of SIF is the key for FM calculations. Owing to the complexities introduced by the structural geometry and the nature of the local stress fields, it is impossible to calculate the SIFs analytically. This problem is often tackled by using simplified models, such as the flat plate solution (Newman and Raju 1986) and methods based on the T-Butt weight function (Chang 1997), with an appropriate load shedding model. The general equation for calculating T-butt *K* value is

$$K = \left[ Mk_m M_m \sigma_m + Mk_b M_b \sigma_b \right] \sqrt{\pi a}$$
(22)

where a is the crack depth, Mk is the weld-toe magnification factor, M is the plain plate shape factor,  $\sigma$  is the nominal plate stress, and subscripts m and b denote membrane and bending loadings, respectively.

According to Lee and Bowness (2002), to approximate the K value for a tubular joint using T-butt solutions, Eq. (22) may be rewritten as Eq. (2) which indicates that the standard stress-life approach may be unconservative for the joints with low DoB values. The reason is that in FM method, despite the stress-life approach, lower DoB may lead to a higher K value and consequently a lower number of cycles to failure (Eq. (20)).

#### 7. Conclusions

Results of 162 stress analyses performed on 81 FE models verified against available experimental data and parametric equations were used to investigate the effects of geometrical parameters on DoB values at saddle and crown positions on the chord-side weld toe of tubular T-joints with concrete-filled chords under axial loadings. A set of DoB parametric equations was also developed for the fatigue design. The key findings can be summarized as follows.

The increase of the  $\beta$  generally results in a decrease in DoB values at the crown position. At the saddle position, the effect of the  $\beta$  on DoB values depends on the axial loading type. Subjected to tension, the increase of the  $\beta$  leads to the decrease of the DoB at the saddle position; while subjected to compression, a regular pattern cannot be identified, and the amount of change is generally not significant.

The increase of the  $\tau$  leads to the decrease of the DoB at the crown position. However, the amount of change is usually small. At the saddle position, the effect of the  $\tau$  on DoB values depends on the axial loading type. Subjected to tension, the increase of the  $\tau$  leads to the decrease of the DoB at the saddle position; while subjected to compression, the increase of the  $\tau$  results in the increase of the DoB at the saddle position. It should also be noted that the amount of DoB change due to the change of the  $\tau$  is generally not significant.

The increase of the  $\gamma$  leads to the increase of the DoB at both crown and saddle positions, and the greatest changes in the DoB due to the change of the  $\gamma$  occur at the saddle position and subjected to tension. The increase of the  $\alpha$  generally leads to the decrease of the DoB at the crown position; but it does not have a considerable effect on the DoB values at the saddle position. At the crown position, the amount of the DoB change due to the change of the  $\alpha$  subjected to compression is more significant compared to tension.

DoB values smaller than 0.8 are frequently observed in axially loaded tubular T-joints with concrete-filled chords. Since the detrimental effect of low DoB on fatigue life has been confirmed, when the standard HSS-based S-N approach is used for the fatigue analysis of axially loaded tubular T-joints with concrete-filled chords, results should be modified to include the effect of the DoB to obtain a more accurate fatigue life prediction.

There can be a quite big difference between the DoB values in tubular T-joints with and without the chord concrete fill. Consequently, developing a set of specific parametric equations for the DoB calculation in T-joints with concrete-filled chords has practical value for design purposes. High coefficients of determination and the satisfaction of acceptance criteria recommended by the UK DoE guarantee the accuracy of the parametric equations proposed in the present paper.

#### References

Ahmadi, H. (2019), "Probabilistic analysis of the DoB in axially-loaded tubular KT-joints of offshore structures", *Appl. Ocean Res.*, **87**, 64-80. https://doi.org/10.1016/j.apor.2019.03.018.

Ahmadi, H. and Alizadeh Atalo, A. (2021), "Geometrical effects on the degree of bending (DoB) of multi-planar tubular KK-joints in jacket substructure of offshore wind turbines", *Appl. Ocean Res.*, **111**, 102678., https://doi.org/10.1016/j.apor.2021.102678.

Ahmadi, H. and Amini Niaki, M. (2019), "Effects of geometrical parameters on the degree of bending (DoB) in two-planar tubular DT-joints of offshore jacket structures subjected to axial and bending loads", *Marine Struct.*, **64**, 229-245. https://doi.org/10.1016/j.marstruc.2018.11.008.

Ahmadi, H. and Asoodeh, S. (2015), "Degree of bending (DoB) in tubular KT-joints of jacket structures

- subjected to axial loads", Int. J. Mar. Tech., 4, 65-75.
- Ahmadi, H. and Asoodeh, S. (2016), "Parametric study of geometrical effects on the degree of bending (DoB) in offshore tubular K-joints under out-of-plane bending loads", Appl. Ocean Res., 58, 1-10. https://doi.org/10.1016/j.apor.2016.03.004.
- Ahmadi, H. and Ghaffari, A.R. (2015a), "Probabilistic analysis of stress intensity factor (SIF) and degree of bending (DoB) in axially loaded tubular K-joints of offshore structures", Lat. Am. J. Solids Struct., 12, 2025-2044. https://doi.org/10.1590/1679-78251698.
- Ahmadi, H. and Imani, H. (2022), "SCFs in offshore two-planar tubular TT-joints reinforced with internal ring stiffeners", Ocean Syst. Eng., 12(1), 1-22, https://doi.org/10.12989/ose.2022.12.1.001.
- Ahmadi, H. and Ghaffari, A.R. (2015b), "Probabilistic assessment of degree of bending (DoB) in tubular X-joints of offshore structures subjected to bending loads", Adv. Civ. Eng., 1-12, https://doi.org/10.1155/2015/518450.
- Ahmadi, H. and Zavvar, E. (2016), "The effect of multi-planarity on the SCFs in offshore tubular KT-joints subjected to in-plane and out-of-plane bending loads", Thin-Wall. Struct., 106, 148-165. https://doi.org/10.1016/j.tws.2016.04.020.
- Ahmadi, H. and Zavvar, E. (2020), "Degree of bending (DoB) in offshore tubular KT-joints under the axial, in-plane bending (IPB), and out-of-plane bending (OPB) loads", Appl. Ocean Res., 95, 102015. https://doi.org/10.1016/j.apor.2019.102015.
- Ahmadi, H., Chamani, S. and Kouhi, A. (2020), "Effects of geometrical parameters on the degree of bending (DoB) in multi-planar tubular XT-joints of offshore structures subjected to axial loading", Appl. Ocean Res., 104, 102381. https://doi.org/10.1016/j.apor.2020.102381.
- Ahmadi, H. and Ghorbani, M. (2023), "Effects of geometrical parameters on the degree of bending in two-planar tubular DYT-joints of offshore jacket structures", Ocean Syst. Eng., 13(2), 97-121. https://doi.org/10.12989/ose.2023.13.2.097.
- Ahmadi, H., Lotfollahi-Yaghin, M.A. and Asoodeh, S. (2015), "Degree of bending (DoB) in tubular K-joints of offshore structures subjected to in-plane bending (IPB) loads: Study of geometrical effects and parametric formulation", Ocean Eng., 102, 105-116, https://doi.org/10.1016/j.oceaneng.2015.04.050.
- Ahmadi, H., Lotfollahi-Yaghin, M.A., Shao, Y.B. and Aminfar, M.H. (2012), "Parametric study and formulation of outer-brace geometric stress concentration factors in internally ring-stiffened tubular KT-joints of offshore structures", Appl. Ocean Res., 38, 74-91. https://doi.org/10.1016/j.apor.2012.07.004.
- Ahmadi, H. and Mohammadpourian Janfeshan, N. (2021), "Local joint flexibility of multi-planar tubular TT-joints: Study of geometrical effects and the formulation for offshore design practice", Appl. Ocean Res., 113, 102758. https://doi.org/10.1016/j.apor.2021.102758.
- Ahmadi, H. and Ziaei Nejad, A. (2017a), "A study on the local joint flexibility (LJF) of two-planar tubular DK-joints in jacket structures under in-plane bending loads", Appl. Ocean Res., 64, 1-14. https://doi.org/10.1016/j.apor.2017.02.002.
- Ahmadi, H. and Ziaei Nejad, A. (2017b), "Local joint flexibility of two-planar tubular DK-joints in OWTs subjected to axial loading: Parametric study of geometrical effects and design formulation", Ocean Eng., 136, 1-10. https://doi.org/10.1016/j.oceaneng.2017.03.011.
- American Petroleum Institute (2007), "Recommended practice for planning, designing and constructing fixed offshore platforms: Working stress design: RP 2A-WSD", 21st Edition, Errata and Supplement 3, Washington DC, US.
- American Welding Society (2002), "Structural welding code: AWS D 1.1", Miami (FL), US.
- Azari-Dodaran, N., Ahmadi, H. and Lotfollahi-Yaghin, M.A. (2018), "Parametric study on structural behavior of offshore tubular K-joints under axial loading at fire-induced elevated temperatures", Thin-Wall. Struct., 130, 467-486. https://doi.org/10.1016/j.tws.2018.06.014.
- Azari-Dodaran, N. and Ahmadi, H. (2019), "Static behavior of two-planar tubular KT-joints under axial fire-induced elevated temperatures", J. Ocean Eng. Sci., https://doi.org/10.1016/j.joes.2019.05.009.
- Bomel Consulting Engineers (1994), "Assessment of SCF equations using Shell/KSEPL finite element data", C5970R02.01 REV C.

- Chang, E. (1997), "Parametric study of non-destructive fatigue strength evaluation of offshore tubular welded joints", PhD Thesis, University College London, UK.
- Chang, E. and Dover, W.D. (1999), "Prediction of degree of bending in tubular X and DT joints", *Int. J. Fatigue*, **21**, 147-161. https://doi.org/10.1016/S0142-1123(98)00060-7.
- Chang, E. and Dover, W.D. (1996), "Stress concentration factor parametric equations for tubular X and DT joints", *Int. J. Fatigue*, **18**, 363-387. https://doi.org/10.1016/0142-1123(96)00017-5.
- Connolly, M.P.M. (1986), "A fracture mechanics approach to the fatigue assessment of tubular welded Y and K-joints", PhD Thesis, University College London, UK.
- Det Norske Veritas (2005), "Fatigue design of offshore steel structures", Recommended Practice, DNV RP C203, Norway.
- Det Norske Veritas (2008), "Structural design of offshore units (WSD method)", Offshore Standard, DNV OS C201, Norway.
- Efthymiou, M. (1988), "Development of SCF formulae and generalized influence functions for use in fatigue analysis", OTJ 88, Surrey, UK.
- Eide, O.I., Skallerud, B. and Berge, S. (1993), "Fatigue of large scale tubular joints-effects of sea water and spectrum loading", *Proceedings of the Fatigue under Spectrum Loading and in Corrosive Environments Conference*, Technical University of Denmark, Lyngby, Denmark.
- Lee, M.M.K. and Bowness, D. (2002), "Estimation of stress intensity factor solutions for weld toe cracks in offshore tubular joints", *Int. J. Fatigue*, **24**, 861-875. https://doi.org/10.1016/S0142-1123(01)00209-2.
- Lie, S.T., Lee, C.K. and Wong, S.M. (2001), "Modeling and mesh generation of weld profile in tubular Y-joint", *J. Const. Steel Res.*, **57**, 547-567. https://doi.org/10.1016/S0143-974X(00)00031-6.
- Morgan, M.R. and Lee, M.M.K. (1998), "Prediction of stress concentrations and degrees of bending in axially loaded tubular K-joints", *J. Const. Steel Res.*, **45**, 67-97. https://doi.org/10.1016/S0143-974X(97)00059-X.
- Musa, I.A., Mashiri, F.R., Zhu, X. and Tong, L. (2018), "Experimental stress concentration factor in concrete-filled steel tubular T-joints", *J. Const. Steel Res.*, **150**, 442-451. https://doi.org/10.1016/j.jcsr.2018.09.001.
- Nassiraei, H. (2019), "Local joint flexibility of CHS X-joints reinforced with collar plates in jacket structures subjected to axial load", *Appl. Ocean Res.*, **93**, 101961. https://doi.org/10.1016/j.apor.2019.101961.
- Nassiraei, H. (2020a), "Geometrical effects on the LJF of tubular T/Y-joints with doubler plate in offshore wind turbines", *Ships Offshore Struct.*, **17**, 481-491. https://doi.org/10.1080/17445302.2020.1835051.
- Nassiraei, H. (2020b), "Local joint flexibility of CHS T/Y-connections strengthened with collar plate under in-plane bending load: Parametric study of geometrical effects and design formulation", *Ocean Eng.*, **202**, 107054. https://doi.org/10.1016/j.oceaneng.2020.107054.
- Nassiraei, H. (2023), "Probability distribution models for the ultimate strength of tubular T/Y-joints reinforced with collar plates at room and different fire conditions", *Ocean Eng.*, **270**, 113557. https://doi.org/10.1016/j.oceaneng.2022.113557.
- Nassiraei, H. (2024a), "Probabilistic analysis of strength in retrofitted X-joints under tensile loading and fire conditions", *Buildings*, **14**, 2105. https://doi.org/10.3390/buildings14072105.
- Nassiraei, H. (2024b), "Probability distribution functions for the ultimate strength of X-joints with collar plates in compressive load at room and fire conditions", *Struct.*, **59**, 105703, https://doi.org/10.1016/j.istruc.2023.105703.
- Nassiraei, H. (2025), "Identification of the most suitable probability models for local joint flexibility in T/Y-connections stiffened with collar or doubler plates", *Results Eng.*, **25**, 104387. https://doi.org/10.1016/j.rineng.2025.104387.
- Nassiraei, H. and Arab, M. (2024), "Compressive load capacity of CHS X-joints: The Efficacy of doubler plates, *Mar. Struct.*, **97**, 103638. https://doi.org/10.1016/j.marstruc.2024.103638.
- Nassiraei, H., Asgarian, B. and Rezadoost, P. (2025a), "Degree of bending in X-connections retrofitted with different types of fiber-reinforced polymers subjected to axial load", *Struct.*, **71**, 107964. https://doi.org/10.1016/j.istruc.2024.107964.

- Nassiraei, H., Chavoshi, H.R. and Talatahari, S. (2025b), "LJF of thin-walled gapped uni-planar K-type tubular steel joints with collar under brace balanced axial loads", Mar. Struct., 99, 103713. https://doi.org/10.1016/j.marstruc.2024.103713.
- Nassiraei, H. and Yara, A. (2022), "Numerical analysis of local joint flexibility of K-joints with external plates under axial loads in offshore tubular structures", J. Mar. Sci. Appl., 21, 134-144. https://doi.org/10.1007/s11804-022-00302-w.
- Nassiraei, H. and Yara, A. (2023), "Static strength of tubular K-joints reinforced with outer plates under axial loads at ambient and fire conditions", Metals, 13, 1857 https://doi.org/10.3390/met13111857.
- Nassiraei, H., Zhu, L. and Gu, C. (2019), "Static capacity of collar plate reinforced tubular X-connections subjected to compressive loading: study of geometrical effects and parametric formulation", Ships Offshore Struct., 16, 54-69. https://doi.org/10.1080/17445302.2019.1708041.
- Newman, J.C. and Raju, I.S. (1986), "Stress intensity factors equations for cracks in three dimensional finite bodies subjected to tension and bending loads", Proceedings of the Conference on Computational Methods in the Mechanics of Fracture, Amsterdam, Netherlands.
- Paris, P. and Erdogan, F. (1963), "A critical analysis of crack propagation laws", J. Basic Eng., 85, 528-534. https://doi.org/10.1115/1.3656900.
- Sadat Hosseini, A., Zavvar, E. and Ahmadi, H. (2021), "Stress concentration factors in FRP-strengthened steel tubular KT-joints", Appl. Ocean Res., 108, 102525. https://doi.org/10.1016/j.apor.2021.102525.
- Shao, Y.B. (2006), "Analysis of stress intensity factor (SIF) for cracked tubular K-joints subjected to balanced axial load", Eng. Fail. Anal., 13, 44-64. https://doi.org/10.1016/j.engfailanal.2004.12.031.
- Shen, W. and Choo, Y.S. (2012), "Stress intensity factor for a tubular T-joint with grouted chord", Eng. Struct., 35, 37-47. https://doi.org/10.1016/j.engstruct.2011.10.014.
- Smedley, P. and Fisher, P. (1991), "Stress concentration factors for simple tubular joints", Proceedings of the International Offshore and Polar Engineering Conference (ISOPE), Edinburgh.
- UK Department of Energy (1983), "Background notes to the fatigue guidance of offshore tubular joints", UK DoE, London, UK.
- Zhao, X.L., Herion, S., Packer, J.A., Puthli, R.S., Sedlacek, G., Wardenier, J., Weynand, K., van Wingerde, A.M. and Yeomans, N.F. (2001), "Design guide for circular and rectangular hollow section welded joints under fatigue loading", CIDECT and TÜV-Verlag, Germany.

# **Nomenclature**

α	Crack size	T	Chord wall thickness
d	Outer diameter of the brace	$X_{\perp}$	Direction perpendicular to the weld toe
D	Outer diameter of the chord	α	Chord slenderness ratio (=2L/D)
DoB	Degree of bending	$\alpha_B$	Brace slenderness ratio (=2l/d)
DoE	Department of Energy	β	Brace-to-chord diameter ratio (=d/D)
FE	Finite elements	γ	Chord wall slenderness ratio (= $D/2T$ )
FM	Fracture mechanics	$\psi$	Dihedral angle
g	Gap	v	Poisson's ratio
HSS	Hot-spot stress	$\sigma_{\scriptscriptstyle B}$	Bending stress
IPB	In-plane bending	$\sigma_{ot W}$	Extrapolated geometric stress at the weld toe
K	Stress intensity factor	$\sigma_{\!\scriptscriptstyle M}$	Membrane stress
L	Chord length	$\sigma_n$	Nominal stress
LJF	Local joint flexibility	$\sigma_{\!\perp\scriptscriptstyle E}$	Stress at an extrapolation point perpendicular
			to the weld toe
OPB	Out-of-plane bending	$\sigma_I$	Weld-toe HSS on the inner surface of the
			chord
$R^2$	Coefficient of determination	$\sigma_{\scriptscriptstyle O}$	Weld-toe HSS on the outer surface of the
			chord
SCF	Stress concentration factor	τ	Brace-to-chord thickness ratio (=t/T)
SIF	Stress intensity factor	$\theta$	Brace inclination angle
t	Brace wall thickness	ζ	Relative gap $(=g/D)$